PHYSICAL REVIEW A VOLUME 22, NUMBER 3 SEPTEMBER 1980

Scattering and spectroscopy: Relativistic multichannel quantum-defect theory

C. M. Lee*
Laboratory for Laser Energetics, University of Rochester, Rochester, New York 14627

W. R. Johnson
Department of Physics, University of Notre Dame, Notre Dame, Indiana 46556

(Received 10 March 1980)

A formulation of relativistic multichannel quantum-defect theory is presented. The relativistic random-phase approximation is applied to calculate the eigenchannel parameters in the relativistic multichannel quantum-defect theory. The resonances due to inner-shell ($1s$) excitations below the K threshold for ions of the Be isoelectronic sequence are studied as illustrative examples.

I. INTRODUCTION

During the past decade there has been an increasing interest in the spectroscopy of atoms and ions of high nuclear charge. This interest arises because of the importance of highly charged ions in the physics of solar flares,[1] tokamak plasmas,[2] and laser-produced laboratory plasmas.[3] Laboratory measurements of the spectra and transition probabilities of highly stripped ions are made using accelerator beam-foil spectroscopy,[4] while neutral atoms of high nuclear charge are studied using synchrotron radiation.[5]

The theoretical methods that have been developed to understand and correlate the atomic data for highly charged atoms and ions have been based on the Dirac equation, since relativistic effects are important for systems in which αZ (Z being the nuclear charge) is not small. For complex atoms electron-electron correlation is also important, and a proper theoretical description of complex high-Z atoms must include both relativity and correlations.

Many of the features of complex atomic spectra can be understood in terms of a few important dynamical parameters using formal scattering theory.[6] One modern approach to scattering theory especially well suited to the description of single-electron ionization is the multichannel quantum-defect theory (MQDT).[7] In the recent past MQDT has been applied to investigate the complex spectra of atoms ranging from He to Ba,[8] and to describe photoelectron angular distributions[9] and spin polarization.[10] The MQDT has also been used to study molecular photoabsorption[11] and to estimate dissociative recombination cross sections between electrons and molecular ions.[12] In view of the many successes of MQDT in correlating atomic data for nonrelativistic systems, it is appropriate to consider a relativistic generalization designed to treat highly charged systems. The purpose of the present paper is to introduce such a generalization and to illustrate how the resulting theory is applied by giving a practical example.

The MQDT provides a detailed description of photoexcitation processes in terms of a relatively small number of parameters. Although these parameters may be obtained empirically, in the present paper we use MQDT in conjunction with a specific dynamical theory to obtain *ab initio* values of the MQDT parameters. In the present study we employ the relativistic random-phase approximation[13] (RRPA) to work out the dynamics. The RRPA has been applied successfully to study photoexcitation and photoionization of highly charged atoms. Applications have been made to the excitation of levels in closed-shell atoms of various isoelectronic sequences.[14] Oscillator strengths for transitions from the ground states to excited states of ions in these sequences are in excellent agreement with more sophisticated many-body calculations.[15]

Cross sections and angular-distribution parameters for photoionization of the closed-shell atoms of He, Be (Ref. 16), Ne, Ar, Kr, and Xe (Ref. 17) have been determined using RRPA.[18] For the lighter elements the RRPA calculations are in close agreement with nonrelativistic RPA calculations[19] and with other nonrelativistic many-body calculations.[20] For the heavier elements Kr and Xe, significant relativistic effects on angular distributions,[21] branching ratios,[22] and spin-polarization parameters[23] are found experimentally; these relativistic effects are explained by RRPA calculations[18,24]. Such applications have been concerned with the average behavior of photoionization cross sections; resonances have been either treated approximately[13] or completely neglected. The practical difficulties which the RRPA shares with other many-body theories are often connected with techniques for extracting information concerning highly excited bound states and resonances; the MQDT provides the proper theoretical framework for treating such questions.

In Sec. II we discuss in detail the relativistic

version of MQDT in which the basic quantum-defect parameters are defined and related to the photoabsorption spectrum. The theory presented in Sec. II is similar to the nonrelativistic MQDT, so we concentrate our attention on those details where the relativistic and nonrelativistic versions differ.

Section III is devoted to a brief outline of the RRPA. To extract the dynamical MQDT parameters, it is particularly convenient to approach RRPA from the time-dependent Hartree-Fock (TDHF) point of view. We discuss the RRPA in terms of TDHF equations for perturbed electronic orbitals, and we show how to determine the MQDT parameters from solutions to the TDHF equations. A reader interested only in the relativistic MQDT, and not in the dynamical model employed here, may skip Sec. III without loss of continuity.

We turn to an illustrative example in Sec. IV. This example is a detailed study of the location and shape of inner-shell $1s \rightarrow np$ resonances along the Be isoelectronic sequence. In neutral Be and in ions of low nuclear charge, the $J^\pi = 1^-$ spectrum consists of a series of $(1s\,2s^2np)\,{}^1P$ resonances; the corresponding ${}^3P$ resonances do not show up in the absorption spectrum because of spin selection rules. By contrast, for Be-like Mo^{38+}, where relativistic effects are important, both the ${}^1P$ and ${}^3P$ resonances are prominent. Since we use a relativistic description throughout, we are able to follow the appearance and development of the forbidden excitations as Z increases along the Be isoelectronic sequence. To put our work in perspective we make comparisons with experimental measurements of inner-shell absorption spectra in the case of neutral Be. We obtain fair agreement between the theoretical and experimental determination of the very narrow resonance lines. For the higher-Z ions considered in Sec. IV (Ne^{6+} and Mo^{38+}), no experimental values are available; however, we expect that, since correlations are less important for higher-Z ions, the predicted spectra of the highly charged ions are at least as accurate as those for neutral Be.

In a subsequent paper[26] these relativistic MQDT techniques are applied to study Beutler-Fano autoionization resonances in the rare gases Ar, Kr, and Xe, and good agreement with recent experimental determinations[27] of the line profiles is obtained. An application of the relativistic MQDT to the autoionization resonances[28] in Ne near 575 Å has already appeared.[29]

II. RELATIVISTIC MULTICHANNEL QUANTUM-DEFECT THEORY

Let us consider an excited atomic system having angular momentum J and parity π with energy below the double-ionization threshold. This excited system consists of a probing (excited bound or excited continuum) electron and a residual ion of charge ζe; the ion itself may of course have various degrees of excitation.

The character of interaction between the probing electron and the ion varies over a range of distances. At large distances the interaction is governed by the static Coulomb potential $-\zeta e^2/r$. Stationary states are represented by linear combinations of electron-ion states combined to give angular momentum J, parity π. Each combination identifies a possible mode of dissociation and is called a dissociation channel, labeled by an index i. Asymptotically, the probing electron is described by a single Dirac orbital in the relativistic theory, viz,

$$u_i(\vec{r}) = \frac{1}{r}\begin{bmatrix} iG_i(r)\Omega_{\kappa_i m_i}(\hat{r}) \\ F_i(r)\Omega_{-\kappa_i m_i}(\hat{r}) \end{bmatrix}, \tag{1}$$

where κ_i and m_i are angular-momentum quantum numbers; $\kappa_i = \mp(j_i + \frac{1}{2})$ for $j_i = l_i \pm \frac{1}{2}$ ($\kappa_i = -1, 1, -2, 2, \ldots$, corresponds to the spectroscopic notation $s_{1/2}, p_{1/2}, p_{3/2}, d_{3/2}, \ldots$). The symbol $\Omega_{\kappa_i m_i}$ designates a spherical spinor, while G_i and F_i are large and small component radial functions. In the sequel we use the abbreviated notation

$$y_i = \begin{bmatrix} G_i \\ F_i \end{bmatrix}$$

for the radial Dirac functions.

At small distances the probing electron and the atomic ion form a complex through which energy and angular momentum can be exchanged. Complicated interactions take place between the electron and ion, requiring an elaborate many-electron theory; in Sec. III we apply RRPA to solve the many-electron problem.

Outside the reaction zone, the radial wave function y of the excited electron orbital for a dissociation channel satisfies a radial Dirac equation

$$Hy = \epsilon y,$$

with

$$H = \begin{bmatrix} m + \frac{\alpha\zeta}{r} & \frac{d}{dr} - \frac{\kappa}{r} \\ -\frac{d}{dr} - \frac{\kappa}{r} & -m + \frac{\alpha\zeta}{r} \end{bmatrix}, \tag{2}$$

where ϵ is the orbital energy, including rest energy m. We use natural units ($\hbar = c = 1$) unless otherwise noted. The radial wave function y is expressed as a linear combination of independent relativistic Coulomb wave functions[30] (f, g),

$$y = af + bg, \tag{3}$$

where a and b are as yet undetermined constants. These relativistic Coulomb wave functions have the following properties:

(1) The pair (f,g) are continuous functions (C^∞ functions) of energy $\epsilon - m$ across the threshold $\epsilon = m$.

(2) At large distances (f,g) have the asymptotic behavior:

(i) For $\epsilon > m$,

$$f \underset{r\to\infty}{\rightarrow} \begin{bmatrix} \left(\frac{\epsilon+m}{\pi p}\right)^{1/2} \cos\left(pr + \frac{\alpha\zeta\epsilon}{p}\ln 2pr - \frac{\pi}{2}(l+1) + \sigma_\kappa^c\right) \\ \left(\frac{\epsilon-m}{\pi p}\right)^{1/2} \sin\left(pr + \frac{\alpha\zeta\epsilon}{p}\ln 2pr - \frac{\pi}{2}(l+1) + \sigma_\kappa^c\right) \end{bmatrix}, \tag{4}$$

and

$$g \underset{r\to\infty}{\rightarrow} \begin{bmatrix} -\left(\frac{\epsilon+m}{\pi p}\right)^{1/2} \sin\left(pr + \frac{\alpha\zeta\epsilon}{p}\ln 2pr - \frac{\pi}{2}(l+1) + \sigma_\kappa^c\right) \\ \left(\frac{\epsilon-m}{\pi p}\right)^{1/2} \cos\left(pr + \frac{\alpha\zeta\epsilon}{p}\ln 2pr - \frac{\pi}{2}(l+1) + \sigma_\kappa^c\right) \end{bmatrix}, \tag{5}$$

with

$$\sigma_\kappa^c = \arg\Gamma(\gamma - i\alpha\zeta\epsilon/p) - \tfrac{1}{2}\pi(\gamma - l - 1) + \eta - \pi s, \tag{6}$$

where

$$s = \tfrac{1}{2}\left(\frac{\kappa}{|\kappa|} + 1\right), \quad \gamma = [\kappa^2 - (\alpha\zeta)^2]^{1/2},$$

$$e^{2i\eta} = \frac{-\kappa + i\alpha\zeta m/p}{\gamma + i\alpha\zeta\epsilon/p},$$

and l is the orbital angular momentum.

(ii) For $\epsilon < m$,

$$f = e^{-i\pi a} y^- - \sin\pi a y^+, \tag{7}$$

$$g = e^{-i\pi(a-1/2)} y^- + \cos\pi a y^+, \tag{8}$$

with

$$a = \gamma + s - \nu, \tag{9}$$

$$\epsilon = \frac{m}{[1 + (\alpha\zeta)^2/\nu^2]^{1/2}}. \tag{10}$$

The parameter ν in Eq. (10) is an "effective" quantum number. Asymptotically,

$$y^- \underset{r\to\infty}{\rightarrow} \left(\frac{1}{2\lambda}\right)^{1/2} \left(\frac{(\nu' - \kappa)}{\Gamma(\nu+\gamma+1)\Gamma(\nu-\gamma+1)}\right)^{1/2} \left(\frac{\sqrt{m+\epsilon}}{\sqrt{m-\epsilon}}\right) (2\lambda r)^\nu e^{-\lambda r}, \tag{11}$$

$$y^+ \underset{r\to\infty}{\rightarrow} \frac{1}{\pi}\left(\frac{1}{2\lambda}\right)^{1/2} \left(\frac{\Gamma(\nu+\gamma+1)\Gamma(\nu-\gamma+1)}{(\nu' - \kappa)}\right)^{1/2} \left(\frac{-\sqrt{m+\epsilon}}{\sqrt{m-\epsilon}}\right) (2\lambda r)^{-\nu} e^{\lambda r}, \tag{12}$$

where

$$\lambda = (m^2 - \epsilon^2)^{1/2} \quad \text{and} \quad \nu' = \alpha\zeta m/\lambda.$$

Each dissociation channel is described in terms of a perturbed radial orbital function in the RRPA, and the dynamics is given by a set of coupled radial differential equations relating the various orbitals. For an M-channel problem there are $2M$ RRPA equations, as shown in Sec. III. The M "negative-frequency" RRPA orbitals (which account for ground-state correlations) are exponentially damped at large distances, while the remaining M "positive-frequency" orbitals (which describe the interchannel interaction including final-state correlations) are required to satisfy stationary-wave asymptotic boundary conditions:

$$y_j^{(i)} \underset{r\to\infty}{\rightarrow} f_j\delta_{ji} + g_j R_{ji}, \quad i,j = 1,\ldots,M. \tag{13}$$

The index j labels the dissociation channels, while the index i distinguishes between the independent solutions to the coupled dynamical equations. The number of independent solutions is just equal to the number of channels. The energy-dependent R matrix is symmetric; it is determined by the solution to the dynamical equations.

Let $U_{i\alpha}$ be the orthogonal matrix of eigenvectors of the matrix R_{ij},

$$\sum_j R_{ij} U_{j\alpha} = \lambda_\alpha U_{i\alpha}, \quad i = 1,\ldots,M \tag{14}$$

and introduce the eigen-quantum defects μ_α by $\lambda_\alpha = \tan\pi\mu_\alpha$. The quantities $\pi\mu_\alpha$ are just the scattering phase shifts when all channels are open. We construct eigenchannel orbitals as linear combinations of the stationary solutions (13):

$$z_j^\alpha = \sum_i U_{i\alpha} \cos\pi\mu_\alpha y_j^{(i)},$$

$$\underset{r\to\infty}{\rightarrow} U_{j\alpha}(f_j \cos\pi\mu_\alpha + g_j \sin\pi\mu_\alpha), \quad j = 1,\ldots,M. \tag{15}$$

The eigenchannel solutions from Eqs. (15), the matrix $U_{i\alpha}$, and the eigen-quantum defects μ_α are only weakly energy dependent. The final physical boundary conditions are expressed in terms of these eigenchannel orbitals.

Physically acceptable solutions to the dynamical

equations are given by a superposition of eigenchannel orbitals:

$$y_j = \sum_\alpha A_\alpha z_j^\alpha, \quad j = 1, \ldots, M \tag{16}$$

with mixing coefficients A_α determined by the boundary conditions. These boundary conditions differ for different ranges of the spectrum, namely, the discrete spectrum, the autoionizing spectrum, and the continuum. The mixing coefficients A_α are functions of the eigenchannel parameters $U_{i\alpha}$ and μ_α and of the energy of the excited system. The transition amplitude in the αth eigenchannel is represented by a reduced matrix element between the initial-state orbitals and those of the αth eigenchannel. Here, since we focus our attention on dipole excitations, we must consider the reduced matrix elements of the dipole operator D_α as additional eigenchannel parameters.

A. Discrete spectrum

The total energy of the excited atomic system is defined with respect to the ground-state energy of the ion by

$$E = E_i + \epsilon_i - m = E_i + \frac{m}{[1+(\alpha\zeta)^2/\nu_i^2]^{1/2}} - m, \quad i = 1, \ldots, M \tag{17}$$

where E_i is the excitation energy of the ion in the ith dissociation channel. For $\alpha\zeta \ll 1$, Eq. (17) reduces to the familiar Rydberg formula. Each E corresponds to a set of numbers ν_i; the number of different ν_i equals the number K of nondegenerate states of the atomic ion. Equations (17) represent a set of $K-1$ independent equations of K unknowns ν_i.

In the discrete spectrum, all dissociation channels are closed, and the boundary conditions that $y_i \to 0$ as $r \to \infty$ for all $j = 1, \ldots, M$ lead to the following set of M equations:

$$\sum_\alpha F_{i\alpha} A_\alpha = 0, \quad i = 1, \ldots, M \tag{18}$$

with

$$F_{i\alpha} = U_{i\alpha} \sin\pi(a_i - \mu_\alpha). \tag{19}$$

The system of linear equations [Eq. (19)] has the compatibility condition

$$F(\{\nu\}) = \det|F_{i\alpha}| = 0 \tag{20}$$

and the nontrival solutions

$$A_\alpha = C_{i\alpha} \Big/ \left(\sum_\alpha C_{i\alpha}^2\right)^{1/2}, \tag{21}$$

where $C_{i\alpha}$ is the cofactor of the element $F_{i\alpha}$ of the determinant $|F_{i\alpha}|$, and the choice of the index i is arbitrary. Solutions to Eqs. (17) and (20), i.e., discrete sets of the numbers $\{\nu_i\}$, give discrete energy levels of the perturbed Rydberg series. For the nth state $\{\nu_i^n\}$, the oscillator strength is expressed as

$$f_n = \tfrac{2}{3}\omega \left|\sum_\alpha A_\alpha^n D_\alpha\right|^2 \Big/ N_n^2, \tag{22}$$

where ω is the photon energy in atomic units and D_α is the reduced dipole matrix element. The normalization factor (in atomic units) is

$$\begin{aligned} N_n^2 &= \sum_i \int_0^\infty dr\, y_i^+ y_i (\alpha\zeta)^2 \\ &= \frac{(\alpha\zeta)^2}{\pi} \sum_i \left[\frac{d}{dE}\left(-\sum_\alpha U_{i\alpha}\sin\pi(a_i-\mu_\alpha)A_\alpha\right)\right]_{E=E_n} \left(\sum_\alpha U_{i\alpha}\cos\pi(a_i-\mu_\alpha)A_\alpha^n\right) \\ &= \sum_i \nu_i^3 \left[1+\left(\frac{\alpha\zeta}{\nu_i}\right)^2\right]^{3/2} \left(\sum_\alpha U_{i\alpha}\cos\pi(a_i-\mu_\alpha)A_\alpha^n\right)^2 \\ &\quad + \sum_\alpha \left(\frac{d\mu_\alpha}{dE}\right)_{E_n} (A_\alpha^n)^2 + \sum_i \sum_\alpha \sum_{\alpha'} \left(\frac{dU_{i\alpha}}{dE}\right)_{E_n} U_{i\alpha'} \sin\pi(\mu_\alpha - \mu_{\alpha'}) A_\alpha^n A_{\alpha'}^n . \end{aligned} \tag{23}$$

B. Autoionization spectrum

In the autoionization spectrum, some dissociation channels are closed and other channels are open. Let us denote Q as the set of the closed dissociation channels and P as the set of the open dissociation channels. Further, let us define P_k as the set of the open dissociation channels pertaining to the kth state of the residual atomic ion. The union of the sets P_k equals the set of P. The number of members of the set P is the number of the open dissociation channels N_P, and the number of members at Q is the number of the closed dissociation channels $N_Q (N_P + N_Q = N)$, where N is the total number of relevant dissociation channels.

The asymptotic boundary conditions describing stationary-wave functions for autoionizing states are that the components of the wave function, Eq. (16), in the closed channels $i \in Q$ vanish exponentially as $r \to \infty$, and that the components in the open

channel $i \in P$ consist of relativistic Coulomb standing waves with a common phase shift $\pi\tau$. Such conditions lead to

$$\sum_\alpha F_{i\alpha} A_\alpha = 0, \quad \forall i \tag{24}$$

with

$$F_{i\alpha} = \begin{cases} U_{i\alpha} \sin\pi(a_i - \mu_\alpha), & i \in Q \\ U_{i\alpha} \sin\pi(\tau - \mu_\alpha), & i \in P. \end{cases} \tag{25}$$

Existence of nontrival solutions of the system of linear equations, Eq. (24) requires

$$F(\{\nu_i; i \in Q\}, \tau) = \det |F_{i\alpha}| = 0. \tag{26}$$

At each energy in the autoionization spectrum, Eq. (26) has roots τ denoted by $\{\tau_\rho; \rho = 1, \ldots, N_\rho\}$. The index ρ identifies a collisional eigenchannel, and the mixing coefficients A^ρ_α are given by an equation similar to Eq. (21), viz.,

$$A^\rho_\alpha = C_{i\alpha}(\{\nu_i, i \in Q\}, \tau_\rho) \Big/ \left(\sum_\alpha [C_{i\alpha}(\{\nu_i, i \in Q\}, \tau_\rho)]^2\right)^{1/2}. \tag{27}$$

The resulting stationary orbitals behave asymptotically as

$$y^\rho_i = \sum_\alpha A^\rho_\alpha z^\alpha_i \xrightarrow[r\to\infty]{} C^\rho_i(r), \tag{28}$$

where

$$C^\rho_i(r) = \begin{cases} T^\rho_i \left[\begin{array}{l} \left(\dfrac{\epsilon_i + m}{\pi p_i}\right)^{1/2} \cos\left(p_i r + \dfrac{\alpha\zeta\epsilon_i}{p_i} \ln 2p_i r - \dfrac{\pi}{2}(l_i+1) + \sigma^c_i + \pi\tau_\rho\right) \\ \left(\dfrac{\epsilon_i - m}{\pi p_i}\right)^{1/2} \sin\left(p_i r + \dfrac{\alpha\zeta\epsilon_i}{p_i} \ln 2p_i r - \dfrac{\pi}{2}(l_i+1) + \sigma^c_i + \pi\tau_\rho\right) \end{array}\right] & \text{for } i \in P \\ \left(\sum_\alpha U_{i\alpha} \cos\pi(a_i - \mu_\alpha) A^\rho_\alpha\right) y^-_i \quad \text{for } i \in Q, \end{cases} \tag{29}$$

with

$$T^\rho_i = \sum_\alpha U_{i\alpha} \cos\pi(\tau_\rho - \mu_\alpha) A^\rho_\alpha. \tag{30}$$

The normalization for the collisonal channel ρ is given by

$$\bar{y}^\rho_i = y^\rho_i / N_\rho, \tag{31}$$

with

$$N_\rho = \left(\sum_{i\in P} (T^\rho_i)^2\right)^{1/2}. \tag{32}$$

The normalized matrix

$$\bar{T}^\rho_i = T^\rho_i / N_\rho \tag{33}$$

is an $N_P \times N_P$ orthogonal matrix. The reduced dipole matrix elements D_ρ in the collisional eigenchannels ρ are

$$\bar{D}_\rho = \left(\sum_\alpha A^\rho_\alpha D_\alpha\right) \Big/ N_\rho. \tag{34}$$

In order to obtain the probability of ejection of a photoelectron into any specific open dissociation channel, we then construct a traveling wave function as a superposition of the collisional eigenchannel functions

$$y^{(j-)}_i = \sum_\rho \bar{y}^\rho_i \bar{A}^{(j-)}_\rho, \tag{35}$$

which satisfies the "incoming-wave" boundary condition at infinity that the amplitude of the outgoing-wave vanish in all open channels $i \neq j$. The desired coefficients $\bar{A}^{(j-)}_\rho$ are

$$\bar{A}^{(j-)}_\rho = \bar{T}^\rho_j e^{-i\pi\tau_\rho}. \tag{36}$$

Thus, the oscillator strength density of the photoelectron group pertaining to the kth state of the residual atomic ion is

$$\frac{df_k}{dE} = \tfrac{2}{3}\omega \sum_{i\in P_k} \left| \sum_\rho \bar{A}^{(i-)}_\rho \bar{D}_\rho \right|^2 = \tfrac{2}{3}\omega \sum_{i\in P_k} \sum_\rho \sum_{\rho'} \bar{T}^\rho_i \bar{T}^{\rho'}_i \cos\pi(\tau_\rho - \tau_{\rho'}) \bar{D}_\rho \bar{D}_{\rho'}. \tag{37}$$

The total oscillator strength density is then expressed as

$$\frac{df}{dE} = \sum_k \frac{df_k}{dE} = \tfrac{2}{3}\omega \sum_\rho \bar{D}^2_\rho = \sum_\rho \frac{df^\rho}{dE}, \tag{38}$$

with

$$\frac{df^\rho}{dE} = \tfrac{2}{3}\omega \left(\sum_\alpha A^\rho_\alpha D_\alpha\right)^2 \Big/ N^2_\rho. \tag{39}$$

For applications to electron-atomic ion collisions in the resonance region, we may construct a traveling wave function as a superposition of the collisional eigenchannel wave functions

$$y_i^{(j+)} = \sum_\rho \bar{y}_i^\rho \bar{A}_\rho^{(j+)}, \tag{40}$$

which satisfies the "outgoing-wave" boundary conditions at $r=\infty$ that the amplitude of the incoming-wave vanish in all open channels $i \neq j$. The desired coefficients are

$$\bar{A}_\rho^{(j+)} = \bar{T}_j^\rho e^{i\pi\tau_\rho}. \tag{41}$$

Thus, the short-range scattering matrix element S_{ij}, for total angular momentum J and parity π, is

$$S_{ij} = \sum_\rho \bar{T}_i^\rho e^{i2\pi\tau_\rho} \bar{T}_j^\rho. \tag{42}$$

The full scattering matrix for J^π symmetry is

$$S_{ij} = \exp(i\sigma_i^c)\left(\sum_\rho \bar{T}_i^\rho e^{i2\pi\tau_\rho} \bar{T}_j^\rho\right)\exp(i\sigma_j^c). \tag{43}$$

C. Continuous spectrum

In this energy range, all dissociation channels are open. In order to obtain the probability of ejection of a photoelectron into any specific channel j, the mixing coefficients in Eq. (16) are determined by requiring that the amplitude of the outgoing wave vanish in all channels $i \neq j$, namely,

$$A_\alpha^{(j-)} = U_{j\alpha} e^{-i\pi\mu_\alpha}. \tag{44}$$

The oscillator strength density of the photoelectron group pertaining to the kth state of the atomic ion is

$$\frac{df_k}{dE} = \frac{2}{3}\omega \sum_{i\in P_k} \left| \sum_\alpha A_\alpha^{(j-)} D_\alpha \right|^2$$
$$= \frac{2}{3}\omega \sum_{i\in P_k} \sum_\alpha \sum_{\alpha'} U_{i\alpha} U_{i\alpha'} \cos\pi(\mu_\alpha - \mu'_\alpha) D_\alpha D'_\alpha. \tag{45}$$

The total oscillator strength density is then

$$\frac{df}{dE} = \sum_k \frac{df_k}{dE}$$
$$= \frac{2}{3}\omega \sum_\alpha D_\alpha^2. \tag{46}$$

In the context of electron-ion collision processes, the full scattering matrix for J^π symmetry can be written as

$$S_{ij} = \exp(i\sigma_i^c)\left(\sum_\alpha U_{i\alpha} e^{i2\pi\mu_\alpha} U_{j\alpha}\right)\exp(i\sigma_j^c). \tag{47}$$

III. RELATIVISTIC RANDOM-PHASE APPROXIMATION

The problem outlined in the Introduction requires a solution to the many-body problem to determine the quantum-defect parameters. In this section we describe the RRPA which is an approximate relativistic many-body theory used to study photoexcitation and photoionization of highly charged atoms and ions.

For our present purposes it is convenient to formulate the RRPA in terms of perturbed single-particle orbitals from the TDHF theory.[31] The TDHF equations describe the response of a closed-shell atom to a time-dependent external field, which we take to be the field of photon incident on the atom. Let us suppose that the external time-dependent perturbation is given by the one-electron operator

$$V = \sum_i v_i(t). \tag{48}$$

For a photon field of frequency ω and multipolarity J, M, λ (J and M are the photon angular-momentum quantum numbers and $\lambda = 0$ or 1 for magnetic or electric multipoles, respectively), we may write

$$v(t) = v_+ e^{-i\omega t} + v_- e^{i\omega t}, \tag{49}$$

with

$$v_+ = \vec{\alpha}\cdot\vec{a}^\lambda_{JM}, \quad v_- = v_+^\dagger, \tag{50}$$

where $\vec{a}^\lambda_{JM}$ is the photon multipole vector potential and $\vec{\alpha}$ is the usual Dirac matrix.

The TDHF equations for a closed-shell atom can be written in terms of single-particle orbitals ϕ_j as

$$i\frac{\partial\phi_j}{\partial t} = [h_0 + v(t)]\phi_j + V_{\rm HF}\phi_j, \quad j = 1, \ldots, N. \tag{51}$$

Here, $V_{\rm HF}$ is the Hartree-Fock potential

$$V_{\rm HF}\phi = \sum_j e^2 \int \frac{d^3r'}{R}[(\phi_j^\dagger \phi_j)'\phi - (\phi_j^\dagger \phi)'\phi_j], \tag{52}$$

and

$$h_0 = \vec{\alpha}\cdot\vec{p} + \beta m - e^2 Z/r \tag{53}$$

is a one-electron Dirac Hamiltonian ($\vec{\alpha}$ and β are Dirac matrices). The RRPA equations are obtained from the TDHF approximation by linearizing in powers of the external field.

We let $u_i(\vec{r})$, $i = 1, \ldots, N$ be stationary orbitals for the Dirac-Fock (DF) ground state of an N-electron closed-shell atom. To carry out the linearization we set

$$\phi_j(\vec{r}, t) = u_i(\vec{r}) e^{-i\epsilon_i t}$$
$$+ w_{i+}(\vec{r}) e^{-i(\epsilon_i+\omega)t}$$
$$+ w_{i-}(\vec{r}) e^{-i(\epsilon_i-\omega)t}. \tag{54}$$

In Eq. (54) ϵ_i is the DF eigenvalue for the orbital $u_i(\vec{r})$, and the functions $w_{i\pm}(\vec{r})$ describe the response of the orbital $u_i(\vec{r})$ to the perturbation $v_\pm(t)$. Substituting Eq. (54) into the TDHF equation

(51) and carrying out the linearization procedure, we obtain the inhomogeneous equations

$$(h_0+v_{\rm HF}+\epsilon_i\pm\omega)w_{i\pm}+V_\pm^{(1)}u_i=v_\pm u_i\,,\quad i=1,\ldots,N\,. \tag{55}$$

Here,

$$V_\pm^{(1)}u=\sum_j e^2\int\frac{d^3r'}{R}\{[(u_j^\dagger w_{j\pm})'+(w_{j\mp}^\dagger u_j)']u - (u_j^\dagger u)'w_{j\pm}-(w_{j\mp}^\dagger u)'u_j\} \tag{56}$$

describes the correlations due to the distortion of the DF potential.

A standard method for solving inhomogeneous equations such as those given in Eqs. (55) is to expand in terms of the complete set of solutions to the corresponding homogeneous system. Let us therefore consider the homogeneous equations

$$(h_0+V_{\rm HF}+\epsilon_i\pm\omega)w_{i\pm}+V_\pm^{(1)}u_i=0\,, \tag{57}$$

along with the orthonormality constraint

$$\int d^3r[(w_{i\pm}^\dagger u_j)+(u_i^\dagger w_{j\mp})]=0\,. \tag{58}$$

The solutions of interest to Eqs. (57) are those which have the angular symmetry dictated by the external field $v_\pm$.

Let us specialize to the case of an applied electric dipole field with $J=1$ and $\lambda=1$. Bearing in mind that the index i of the orbital $u_i(\vec{r})$ refers to a set of central-field quantum numbers $i=(n,\kappa,m)$, one readily establishes that the perturbed orbitals $w_{i\pm}$ have angular quantum numbers $\bar{\kappa}=-\kappa$, $\kappa\pm1$. Thus, for example, an unperturbed $d_{3/2}$ orbital with $\kappa=2$ will be excited to states with angular-momentum quantum numbers $\bar{\kappa}=1$, -2, and 3, corresponding to $p_{1/2}$, $p_{3/2}$, and $f_{5/2}$ angular symmetries by the applied dipole field. In our example in Sec. IV the $s_{1/2}$ orbitals of Be-like ions which have $\kappa=-1$ are excited to $p_{1/2}$ and $p_{3/2}$ orbitals with $\bar{\kappa}=1$ and -2, respectively.

Using the standard methods of Racah algebra, we may reduce Eqs. (57) to a set of coupled radial differential equations suitable for computer solution. We let $w_{k\pm}$ be the perturbed orbital (of frequency $\pm\omega$) associated with the excitation k: $(n,\kappa,m)\to(\epsilon,\bar{\kappa},\bar{m})$. In the notation of the previous section, k corresponds to a dissociation channel in which the ion remains in the state $(n,\kappa,-m)$, while the electron is excited to a continuum state $(\epsilon,\bar{\kappa},\bar{m})$. The electron orbital $w_{k\pm}$ can be written

$$w_{k\pm}=\frac{1}{r}\begin{bmatrix}iG_k(r)\Omega_{\bar{\kappa}\bar{m}}(\hat{r})\\ F_k(r)\Omega_{-\bar{\kappa}\,\bar{m}}(\hat{r})\end{bmatrix}\,. \tag{59}$$

We write, following the notation of the previous section,

$$y_{k\pm}=\begin{bmatrix}G_{k\pm}(r)\\ F_{k\pm}(r)\end{bmatrix}\,. \tag{60}$$

To describe the radial functions, we introduce

$$H_{\bar{\kappa}}=\begin{bmatrix}m+V_k(r) & \dfrac{d}{dr}-\dfrac{\bar{\kappa}_k}{r}\\ -\dfrac{d}{dr}-\dfrac{\bar{\kappa}_k}{r} & -m+V_k(r)\end{bmatrix}\,, \tag{61}$$

where $V_k(r)$ is the ion potential. We may then rewrite Eq. (57) as a set of coupled radial equations

$$(H_{\bar{\kappa}}-\epsilon_k\mp\omega)y_{k\pm}=O_{k\pm}\,, \tag{62}$$

where $O_{k\pm}$ is the coupling due to the correlation potential $V_\pm^{(1)}$. The radial equations (62) are written out in detail in Ref. 16.

Solutions to Eqs. (62) are either oscillatory or exponential at large r, depending on whether $\epsilon_k\pm\omega$ is larger or smaller than the electron mass m. The radial function y_{k+} represents the excited electron orbital, and at large distances (where V_k takes on its asymptotic behavior as an ionic Coulomb potential) the orbital y_{k+} is just a linear combination of the Coulomb wave functions given in Eq. (3). The negative-frequency perturbations y_{k-} describe the effects of correlation on the atomic ground state; these negative-frequency perturbed orbitals are always exponentially damped at large r.

The index k ranges over the various possible values of n, k, $\bar{\kappa}$ corresponding to the dipole excitation of an electron to state $\bar{\kappa}$, leaving an ion with a hole in the state n,κ. This is just the set of M dissociation channels of the atom discussed in Sec. II.

The number of equations in the system (62) is $2M$, twice the number of dissociation channels. For the M-negative-frequency orbitals $y_{k-}(r)$, the physically relevant boundary conditions are that the solutions be regular at the origin and exponentially damped at large r [see Eq. (64) below]. The remaining freedom in the solutions to Eqs. (62) is resolved by requiring that the solutions $y_{k+}(r)$ be regular at $r=0$ and satisfy the boundary conditions for perturbed orbitals given in Eq. (13). Thus,

$$y_{k+}^{(i)}\xrightarrow[r\to\infty]{}f_k\delta_{ki}+g_kR_{ki}\,,\quad i,k=1,\ldots,M \tag{63}$$

$$y_{k-}^{(i)}\xrightarrow[r\to\infty]{}0\,,\quad i,k=1,\ldots,M\,. \tag{64}$$

Each value of the index i defines a stationary-wave solution to Eqs. (62), and the symmetric reaction matrix R_{ik} is determined as a function of energy from the solution. The normalization constant for the solutions to Eqs. (62) is given by

$$N^2 = \int dr \sum_k (y_{k+}^2 - y_{k-}^2), \tag{65}$$

as discussed, for example, in Ref. 16. Given a normalized solution to Eqs. (62) one finds the reduced dipole matrix element between a state described by $y_{k\pm}^{(i)}$ and the atomic ground state as

$$D^{(i)} = \sum_k (R_{k+}^{(i)} + R_{k-}^{(i)}), \tag{66}$$

where the radial integrals $R_k^{(i)}$ are given by

$$R_{k\pm}^{(i)} = C(k,\bar{k}) \int dr\, r (G_k G_{k\pm}^{(i)} + F_k F_{k\pm}^{(i)}). \tag{67}$$

In Eq. (67) the symbols G_k, F_k describes the ground-state DF orbitals, while $G_k^{(i)}$ and $F_k^{(i)}$ are the large and small components of the perturbed-orbital solution to Eqs. (62). The angular-momentum factor $C(k,\bar{k})$ in Eq. (67) is

$$C(k,\bar{k}) = \begin{cases} (-1)^{j_k+1/2}[(2j_k+1)(2\bar{j}_k+1)]^{1/2} \begin{pmatrix} j_k & j_k & 1 \\ -\frac{1}{2} & \frac{1}{2} & 0 \end{pmatrix}, & l_k+\bar{l}_k \text{ odd} \\ 0, & l_k+\bar{l}_k \text{ even} \end{cases} \tag{68}$$

where the large round bracket designates a 3-j symbol. The RRPA equations give dipole matrix elements which are identical in length and velocity forms. In the velocity form Eq. (67) is replaced by

$$V_{k\pm}^{(i)} = \pm\frac{1}{\omega} C(k,\bar{k}) \int dr [(\kappa_k - \bar{\kappa}_k)(F_k G_{k\pm}^{(i)} + G_k F_{k\pm}^{(i)}) + (F_k G_{k\pm}^{(i)} - G_k F_{k\pm}^{(i)})]. \tag{69}$$

Dipole matrix elements D_α employed in Sec. II are obtained from Eq. (66) by forming the combinations of $D^{(i)}$ implied by Eq. (15), viz.,

$$D_\alpha = \sum_i D^{(i)} U_{i\alpha} \cos\pi\mu_\alpha. \tag{70}$$

The solution to the problem posed in the Introduction is now completely specified. We first solve Eqs. (62) subject to boundary conditions (63) and (64). The R matrix is then diagonalized to give the quantum-defect parameters μ_α and $U_{i\alpha}$, which are used together with the dipole matrix elements D_α to describe bound states, resonances, and the continuum, according to the method outlined in Sec. II.

IV. APPLICATIONS

As specific examples of the methods developed in the previous sections we consider the $1s \rightarrow np$ autoionization resonances for neutral beryllium and for several ions of the beryllium isoelectronic sequence. In these examples we ignore channels such as $1s\{(2s2p)^{1,3}P\}(^{ns}_{nd})$ associated with two electron excitations, since consideration of these channels requires a dynamical scheme beyond the RPA.[32]

In Table I we compare the calculated resonance positions below the K-shell threshold with the experimental data of Mehlman and Esteva.[25] These experimental data, which were based on synchronous-arc plasma-absorption measurements contain complicated structures due to mixtures of Be atoms, metastable Be atoms, and Be^+ ions. Mehlman and Esteva were able to determine the positions of the inner-shell excited states with high accuracy (±25 meV, i.e., ±0.02 Å). For the first resonance the width can be determined theoretically as $(\Delta\nu)_{1s\rightarrow 2p} = 4.0\times 10^{-5}$, while the experimental measurement is limited by the spectral resolution (±0.02 Å). Part of the disagreement between the experimental and theoretical values shown in Table I is due to the omission of two electron excitations in the theory; another part, we believe, is due to the difficulty in determining the experimental threshold and the consequent loss of significance in determining the different between resonance positions and threshold. The theoretically predicted location of the autoionizing resonances is in agreement with a previous nonrelativistic TDHF calculation by Stewart *et al.*,[33] as is to be expected, since relativistic effects are insignificant for neutral beryllium.

The Be autoionizing sequence is illustrated in Fig. 1, where the predicted oscillator strength distribution is plotted against wavelength. In this figure we use the experimental value of the K threshold given by Mehlman and Esteva, instead of the theoretical RRPA value. The locations of the first three experimental lines are marked on Fig. 1 for comparison.

The evolution of the resonance profiles as Z increases along the isoelectronic sequence is shown in Fig. 2, where we plot theoretical absorption cross

TABLE I. Beryllium autoionizing states $[1s(2s)^2np]^1P$.

State	Expt. energy[a] (cm^{-1})	ν_{expt}[b]	ν_{theor}
$1s(2s)^2 2p$	931 300	1.31	1.27
$1s(2s)^2 3p$	979 200	2.6	2.40
$1s(2s)^2 4p$	988 200	4	3.42

[a] Mehlman and Esteva, Ref. 25.
[b] Based on an experimental threshold of 994 900 cm^{-1}.

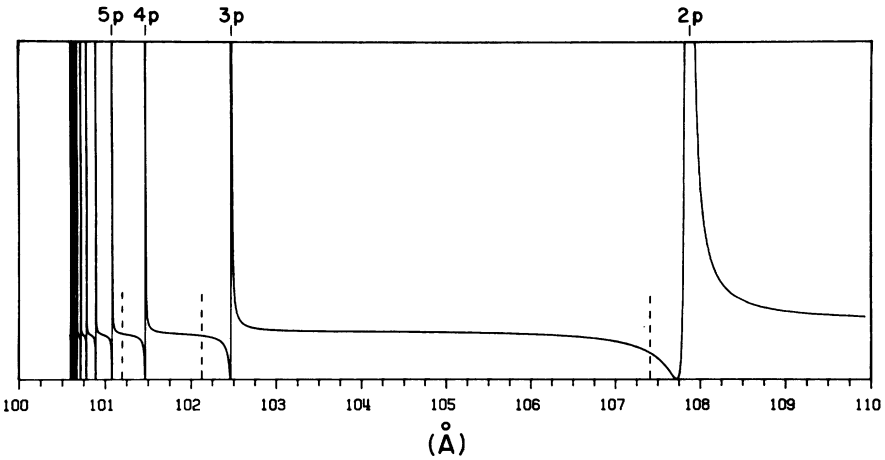

FIG. 1. Theoretical oscillator strength distribution for Be including $1s \rightarrow np$ autoionization resonances. The vertical dashed lines mark the location of experimental resonances (Mehlman and Esteva, Ref. 25).. The experimental threshold at 994 900 cm^{-1} is used.

sections along with the short-range electron-ion scattering phase shift $\pi\tau$. For neutral beryllium, the phase shifts corresponding to the two open channels show resonances $[1s(2s)^2 2p]^3P$ and $[1s(2s)^2 2p]^1P$, $\nu \sim 1.15$ and $\nu \sim 1.27$, respectively. The character of the resonant states, i.e., ^1P and ^3P, is identified by the character of the eigenchannels which represent the dynamics at short range. Because of electron-electron interaction, the ^3P resonance occurs at lower energy than the ^1P resonance. As a consequence of electric dipole selection rules, the photoionization cross section shows only one resonance for neutral Be at the ^1P position.

For the Be-like neon ion Ne^{6+}, the character of the eigenchannels is no longer described by a pure LS coupling scheme. The smaller resonance near $\nu = 1.78$ is dominated by a ^3P state with a small admixture of ^1P character, while the larger resonance near $\nu = 1.81$ is dominantly ^1P with a small mixture of ^3P.

As Z increases the coupling scheme changes from an almost pure LS scheme at neutral Be to a jj scheme for high Z. Indeed, for Be-like Mo^{38+} the eigenchannels are characterized by almost pure jj coupling. The positions of the first two Mo^{38+} resonances differ by $\Delta\nu \sim 0.03$, which is principally due to the spin-orbit difference $\Delta\nu_{so} = \frac{1}{4}(\alpha Z)^2 \sim 0.02$. Furthermore, the strengths of the two resonances are comparable, as a result of jj coupling.

In plotting the open-channel phases in Fig. 2, we have connected the individual phases smoothly through crossing points in the cases of Be and Ne^{6+}; however, our numerical analysis shows that the points of intersection in the figures are actually "anticrossings," as illustrated in the diagram for the Mo^{38+} phase shift.

Finally, we wish to stress that the eigenchannel parameters μ_α, $U_{i\alpha}$, and D_α in the relativistic MQDT can be obtained, as in the nonrelativistic MQDT, either from *ab initio* calculations to treat many-electron dynamics, or from a semiempirical analysis to fit available spectroscopic data. The two approaches complement each other; they may be pursued individually or by a judicious combination of the two approaches, which may prove to be a more satisfactory alternative. To treat open-shell atoms the RRPA dynamics outlined in the previous section is not adequate, and a more sophisticated dynamical scheme is required for the *ab initio* determination of the relativistic MQDT parameters.

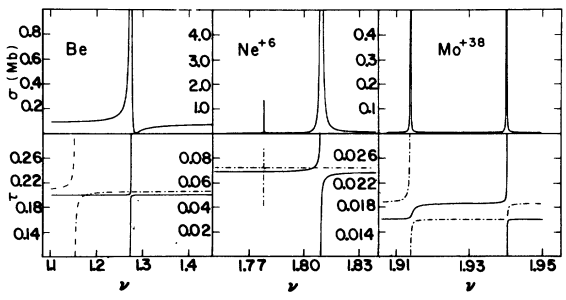

FIG. 2. Absorption cross sections (Mb) and open-channel phases parameters τ (phase $= \pi\tau$) are given in terms of the effective quantum number ν near the $1s \rightarrow 2p$ autoionizing resonances in the 4-electron ions Be, Ne^{6+}, and Mo^{38+}. The broken lines in the lower panels correspond to ^3P states, while the solid lines are for ^1P states.

ACKNOWLEDGMENTS

The authors wish to express their gratitude to Laboratoire pour l'Utilisation du Rayonnement Electromagnétique and Centre Européan De Calcul Atomique et Moleculaire for the arrangement of the workshop on inner-shell excitations of atoms, molecules, and solids, where parts of this work were completed. Thanks are due to Vo Ky Lan at the Observatoire de Paris, Meudon, for his hospitality and to M. LeDourneuf for her help at the Centre Inter-Regional de Calcul Electronique computing facility. The work of W. R. J. was supported in part by the U. S. National Science Foundation. The work of C. M. Lee was partially supported by the Laser Fusion Feasibility Project, which is sponsored by Exxon Research and Engineering Company, General Electric Company, Northeast Utilities Company, Empire State Electric Research Company, and the New York State Energy Research and Development Administration.

---

*Permanent address: Institute of Physics, Academy of Science, Peking, China.

[1]C. Jordan, in *Progress in Atomic Spectroscopy*, Part B, edited by W. Hanle and H. Kleinpoppen (Plenum, New York, 1979), pp. 1453–1483; A. K. Dupree, Adv. At. Mol. Phys. 14, 393 (1978).

[2]E. Hinnov, Phys. Rev. A 14, 1533 (1976); T. F. R. Group, J. Phys. (Paris) C4, 86 (1978).

[3]E. V. Aglitskii, V. A. Boiko, O. N. Krohkin, S. A. Pikuz, and A. Ya. Faenov, Sov. J. Quantum Electron. 4, 1152 (1975); P. G. Burkhalter, J. Reader, and R. D. Cowan, J. Opt. Soc. Am. 67, 1521 (1977).

[4]I. Martinson, in *Beam-Foil Spectroscopy*, edited by S. Bashkin (Springer, Berlin, 1976), pp. 31–61. H. G. Berry, Rep. Prog. Phys. 40, 155 (1977).

[5]K. Codling, in *Synchrotron Radiation, Techniques and Applications*, edited by C. Kunz (Springer, Berlin, 1979), pp. 231–265.

[6]M. L. Goldberger and K. M. Watson, *Collision Theory* (Wiley, New York, 1967), pp. 352 and 375.

[7]M. J. Seaton, Proc. Phys. Soc. London 88, 801 (1966); U. Fano, Phys. Rev. A 2, 353 (1970).

[8]U. Fano, J. Opt. Soc. Am. 65, 979 (1975), a review of work of Fano's group; J. A. Armstrong, P. Esherick, and J. J. Wynne, Phys. Rev. A 15, 180 (1977), a representative work from the IBM group; J. Dubau and J. Wells, J. Phys. B 6, 1452 (1973), a work from Seaton's group devoted to the Be atoms.

[9]D. Dill, Phys. Rev. A 7, 1976 (1973); J. Geiger, Z. Phys. A276, 219 (1976).

[10]C. M. Lee, Phys. Rev. A 10, 1598 (1974).

[11]Ch. Jungen and O. Atabek, J. Chem. Phys. 66, 5584 (1977).

[12]C. M. Lee, Phys. Rev. A 16, 109 (1977).

[13]M. Ya. Amusia and N. A. Cherepkov, Case Stud. At. Phys. 5, 47 (1975), nonrelativistic theory; G. Wendin, in *Vacuum Ultraviolet Radiation Physics*, edited by E. E. Koch, R. Haensel, and C. Kunz (Pergamon, Braunschweig, 1974), p. 225 (nonrelativistic theory); W. R. Johnson, C. D. Lin, K. T. Cheng, and C. M. Lee, Phys. Scr. 21, 409 (1980) (relativistic theory).

[14]W. R. Johnson and C. D. Lin, Phys. Rev. A 14, 565 (1976); C. D. Lin, W. R. Johnson, and A. Dalgarno, *ibid.* 15, 154 (1977); P. Shorer, C. D. Lin, and W. R. Johnson, *ibid.* 16, 1109 (1977); P. Shorer and A. Dalgarno, *ibid.* 16, 1502 (1977); P. Shorer, *ibid.* 18, 1060 (1978).

[15]Y. Accad, C. L. Pekeris, and B. Schiff, Phys. Rev. A 4, 885 (1971); C. M. Moser, R. K. Nesbet, and M. N. Gupta, *ibid.* 13, 17 (1976).

[16]W. R. Johnson and C. D. Lin, J. Phys. B 10, L331 (1077); C. D. Lin and W. R. Johnson, *ibid.* 12, 1677 (1979).

[17]W. R. Johnson and K. T. Cheng, Phys. Rev. A 20, 978 (1979).

[18]W. R. Johnson and C. D. Lin, Phys. Rev. A 20, 964 (1979).

[19]T. N. Chang, Phys. Rev. A 15, 2392 (1977).

[20]H. P. Kelly and R. L. Simons, Phys. Rev. Lett. 30, 529 (1973); P. G. Burke and K. T. Taylor, J. Phys. B 8, 2620 (1975); J. R. Swanson and L. Armstrong, Jr., Phys. Rev. A 16, 1117 (1977).

[21]J. L. Dehmer and D. Dill, Phys. Rev. Lett. 37, 1049 (1976); J. L. Dehmer, W. A. Chupka, J. Berkowitz, and W. T. Jiverey, Phys. Rev. A 12, 1966 (1975); D. L. Miller, J. D. Dow, R. G. Houlgate, G. V. Marr, and J. B. West, J. Phys. B 10, 3205 (1977).

[22]F. Wuilleumier, M. Y. Adam, P. Dhez, N. Sandner, V. Schmidt, and W. Melhorn, Phys. Rev. A 16, 646 (1977).

[23]U. Heinzmann, G. Schönhense, and J. Kessler, Phys. Rev. Lett. 42, 1603 (1979).

[24]K.-N. Huang, W. R. Johnson, and K. T. Cheng, Phys. Rev. Lett. 43, 1658 (1979).

[25]G. Mehlman and J. M. Esteva, Astrophys. J. 188, 191 (1974).

[26]W. R. Johnson, K. T. Cheng, and K.-N. Huang, Phys. Rev. A 22, 989 (1980).

[27]K. Radler and J. Berkowitz, J. Chem. Phys. 70, 221 (1979).

[28]K. Radler and J. Berkowitz, J. Chem. Phys. 70, 216 (1979).

[29]W. R. Johnson and M. LeDourneuf, J. Phys. B 13, L13 (1980).

[30]W. R. Johnson and K. T. Cheng, J. Phys. B 12, 863 (1979).

[31]A. Dalgarno and G. A. Victor, Proc. R. Soc. London A297, 291 (1966).

[32]F. Bely-Dubau, J. Dubau, and D. Petrini, J. Phys. B 10, 1613 (1977).

[33]R. F. Stewart, D. K. Watson, and A. Dalgarno, J. Chem. Phys. 63, 3222 (1975).